

Correspondence

1 Compressive-Sensing-Based Multiuser Detector for the 2 Large-Scale SM-MIMO Uplink

3 Zhen Gao, Linglong Dai, Zhaocheng Wang, *Senior Member, IEEE*,
4 Sheng Chen, *Fellow, IEEE*, and Lajos Hanzo, *Fellow, IEEE*

5 **Abstract**—Conventional spatial modulation (SM) is typically consid-
6 ered for transmission in the downlink of small-scale multiple-input-
7 multiple-output (MIMO) systems, where a single antenna element (AE) of
8 a set of, e.g., 2^P AEs is activated for implicitly conveying p bits. By contrast,
9 inspired by the compelling benefits of large-scale MIMO (LS-MIMO)
10 systems, here, we propose an LS-SM-MIMO scheme for the uplink (UL),
11 where each user having multiple AEs but only a single radio frequency
12 (RF) chain invokes SM for increasing the UL throughput. At the same time,
13 by relying on hundreds of AEs and a small number of RF chains, the base
14 station (BS) can simultaneously serve multiple users while reducing the
15 power consumption. Due to the large number of AEs of the UL users and
16 the comparably small number of RF chains at the BS, the UL multiuser sig-
17 nal detection becomes a challenging large-scale underdetermined problem.
18 To solve this problem, we propose a joint SM transmission scheme and
19 a carefully designed structured compressive sensing (SCS)-based multi-
20 user detector (MUD) to be used at the users and the BS, respectively.
21 Additionally, the cyclic-prefix single carrier (CPSC) is used to combat
22 the multipath channels, and a simple receive AE selection is used for the
23 improved performance over correlated Rayleigh-fading MIMO channels.
24 We demonstrate that the aggregate SM signal consisting of multiple UL
25 users' SM signals of a CPSC block exhibits distributed sparsity. Moreover,
26 due to the joint SM transmission scheme, aggregate SM signals in the same
27 transmission group exhibit group sparsity. By exploiting these intrinsically
28 sparse features, the proposed SCS-based MUD can reliably detect the
29 resultant SM signals with low complexity. Simulation results demonstrate
30 that the proposed SCS-based MUD achieves a better signal detection
31 performance than its counterparts even with higher UL throughput.

32 **Index Terms**—Compressive sensing (CS), large-scale multiple-input-
33 multiple-output (LS-MIMO), multiuser detector (MUD), spatial modula-
34 tion (SM).

35 I. INTRODUCTION

36 A widely recognized consensus is that fifth-generation (5G) sys-
37 tems will be capable of providing significant energy efficiency and
38 system capacity improvements [1], [2]. Promising techniques, such
39 as large-scale multiple-input-multiple-output (LS-MIMO) and spatial
40 modulation (SM)-MIMO systems, are considered as potent candidates
41 for 5G systems [1]–[5]. LS-MIMO employing hundreds of antenna

elements (AEs) at the base station (BS) is capable of improving 42
spectral efficiency by orders of magnitude, but it suffers from the 43
nonnegligible power consumption and hardware cost due to one spe- 44
cific radio frequency (RF) chain usually required by every AE [5]. 45
By using a reduced number of RF chains, the emerging SM-MIMO 46
activates part of available AEs to transmit extra information in the 47
spatial domain, and it has attracted much attention due to its high en- 48
ergy efficiency and reduced hardware cost [5]. However, conventional 49
SM-MIMO is usually considered in the downlink of small-scale 50
MIMO systems, and therefore, its achievable capacity is limited. Indi- 51
vidually, both technologies have their own advantages and drawbacks. 52
By an effective combination of them, one can envision the win-win 53
situation. SM-MIMO is attractive for LS-MIMO systems, since the 54
reduced number of required RF chains in SM-MIMO can reduce the 55
power consumption and hardware cost in conventional LS-MIMO 56
systems. Moreover, hundreds of AEs used in LS-MIMO can im- 57
prove the system throughput of SM-MIMO. Such reciprocity enables 58
LS-MIMO and SM-MIMO to enjoy the apparent compatibility. 59

In this paper, we propose an LS-SM-MIMO scheme for intrinsi- 60
cally amalgamating the compelling benefits of both LS-MIMO and 61
SM-MIMO for the 5G uplink (UL) over frequency-selective fading 62
channels. In the proposed scheme, each UL user equipped with mul- 63
tiple AEs but only a single RF chain invokes SM for increasing the 64
UL throughput, and the cyclic-prefix single-carrier (CPSC) transmis- 65
sion scheme is adopted to combat the multipath channels [6]. At the 66
BS, hundreds of AEs but only dozens of RF chains are employed to 67
simultaneously serve multiple users, and a direct AE selection scheme 68
is used to improve the system performance over correlated Rayleigh- 69
fading MIMO channels at the BS [7]. The proposed scheme can 70
be adopted in conventional LS-MIMO as a specific UL-transmission 71
mode for reducing the power consumption or, alternatively, for energy- 72
and cost-efficient LS-SM-MIMO, where joint benefits of efficient AE 73
selection [7], transmit precoding [8], and channel estimation [9] can 74
be readily exploited. To sum up, the proposed scheme inherits the 75
advantages of LS-MIMO and SM-MIMO, while reducing the power 76
consumption and hardware cost. 77

A challenging problem in the proposed UL LS-SM-MIMO scheme 78
is how to realize a reliable multiuser detector (MUD) with low com- 79
plexity. The optimal maximum likelihood (ML) signal detector suffers 80
from excessive complexity. Conventional sphere decoding detectors 81
cannot be readily used in multiuser scenarios and may still exhibit high 82
complexity for LS-SM-MIMO [10]. Existing low-complexity linear 83
signal detectors, e.g., the minimum mean square error (MMSE)-based 84
signal detector, perform well for conventional LS-MIMO systems 85
[4]. However, they are unsuitable for the proposed LS-SM-MIMO 86
UL transmission, since the large number of transmit AEs of the UL 87
users and the reduced number of receive RF chains at the BS make 88
UL multiuser signal detection a large-scale underdetermined/rank- 89
deficient problem. The authors in [11]–[13] proposed compressive 90
sensing (CS)-based signal detectors to solve the underdetermined 91
signal detection problem in SM-MIMO systems, but they only consid- 92
ered the single-user small-scale SM-MIMO systems in the downlink. 93

Against this background, our new contribution is that we exploit 94
the specific signal structure in the proposed multiuser LS-SM-MIMO 95
UL transmission, where each user only activates a single AE in each 96
time slot. Hence, the SM signal of each UL user is sparse with 97

Manuscript received May 7, 2015; revised October 1, 2015; accepted November 14, 2015. This work was supported in part by the International Science and Technology Cooperation Program of China under Grant 2015DFG12760, by the National Natural Science Foundation of China under Grant 61571270 and Grant 61201185, by the Beijing Natural Science Foundation under Grant 4142027, and by the Foundation of Shenzhen government. The review of this paper was coordinated by Dr. Y. Xin.

Z. Gao, L. Dai, and Z. Wang are with the Tsinghua National Laboratory for Information Science and Technology (TNList), Department of Electronic Engineering, Tsinghua University, Beijing 100084, China (e-mail: gao-z11@mails.tsinghua.edu.cn; daill@mail.tsinghua.edu.cn; zcwang@mail.tsinghua.edu.cn).

S. Chen and L. Hanzo are with the School of Electronics and Computer Science, University of Southampton, Southampton SO17 1BJ, U.K. (e-mail: sqc@ecs.soton.ac.uk; lh@ecs.soton.ac.uk).

Color versions of one or more of the figures in this paper are available online at <http://ieeexplore.ieee.org>.

Digital Object Identifier 10.1109/TVT.2015.2501460

the sparsity level of one, and the aggregate SM signal consisting of multiple UL users' SM signals of a CPSC block exhibits certain distributed sparsity, which can be beneficially exploited for improving the signal detection performance at the BS. Moreover, we propose a joint SM transmission scheme for the UL users in conjunction with an appropriately structured CS (SCS)-based MUD at the BS. The proposed SCS-based MUD is specifically tailored to leverage the inherently distributed sparsity of the aggregate SM signal and the group sparsity of multiple aggregate SM signals, owing to the joint SM transmission scheme for reliable signal detection performance. Our simulation results demonstrate that the proposed SCS-based MUD is capable of outperforming the conventional detectors even with higher UL throughput.

The rest of this paper is organized as follows. Section II introduces the system model of the proposed LS-SM-MIMO scheme. Section III specifies the proposed joint SM transmission and SCS-based MUD. Section IV provides our simulation results. Section V concludes this paper.

Throughout this paper, lowercase and uppercase boldface letters denote vectors and matrices, respectively, whereas $(\cdot)^T$, $(\cdot)^*$, $(\cdot)^\dagger$, and $[\cdot]$ denote the transpose, conjugate transpose, Moore–Penrose matrix inversion, and the integer floor operators, respectively. The l_0 and l_2 norm operations are given by $\|\cdot\|_0$ and $\|\cdot\|_2$, respectively. The support set of vector \mathbf{x} is denoted by $\text{supp}\{\mathbf{x}\}$, and \mathbf{x}_i denotes the i th entry of vector \mathbf{x} . Additionally, $\mathbf{x}|_\Gamma$ denotes the entries of \mathbf{x} defined in the set Γ , $\Phi|_\Gamma$ denotes the submatrix whose columns comprise the 124 columns of Φ that are defined in Γ , and $\Phi|_\Gamma$ denotes the submatrix 125 whose rows comprise the rows of Φ that are defined in Γ . The expectation operator is given by $E\{\cdot\}$. $\text{mod}(x, y) = x - \lfloor x/y \rfloor y$ if $y \neq 0$ and $x - \lfloor x/y \rfloor y \neq 0$, whereas $\text{mod}(x, y) = y$ if $y \neq 0$ and $x - \lfloor x/y \rfloor y = 0$.

II. SYSTEM MODEL

We first introduce the proposed LS-SM-MIMO scheme and then focus our attention on the UL transmission with an emphasis on the multiuser signal detection.

133 A. Proposed Multiuser LS-SM-MIMO Scheme

As shown in Fig. 1, we consider the proposed LS-SM-MIMO from both the BS side and the user side. For conventional LS-MIMO, the number of AEs employed by the BS is equal to the number of its RF chains [4]. However, the BS in LS-SM-MIMO, as shown in Fig. 1, is equipped with a much smaller number of RF chains M_{RF} than the total number of AEs M , i.e., we have $M_{\text{RF}} \ll M$. Conventional LS-MIMO systems typically assume single-antenna users [4]. By contrast, in the proposed scheme, each user is equipped with $n_t > 1$ AEs but only a single RF chain, and SM is adopted for the UL transmission, where only one of the available AEs is activated for data transmission. It has been shown that the main power consumption and hardware cost of cellular networks comes from the radio access network [1]. Hence, using a reduced number of expensive RF chains compared with the total number of AEs at the BS can substantially reduce both the power consumption and the hardware cost for the operators. Meanwhile, it is feasible to incorporate several AEs and a single RF chain in the handsets. The resultant increased degrees of freedom in the spatial domain may then be exploited for improving the UL throughput. The proposed scheme can be considered as an optional UL-transmission mode in conventional LS-MIMO systems, where AE selection schemes may be adopted for beneficially selecting the most suitable M_{RF} AEs at the BS to receive UL SM signals [7]. Alternatively, it can also be used for the UL of LS-SM-MIMO, when

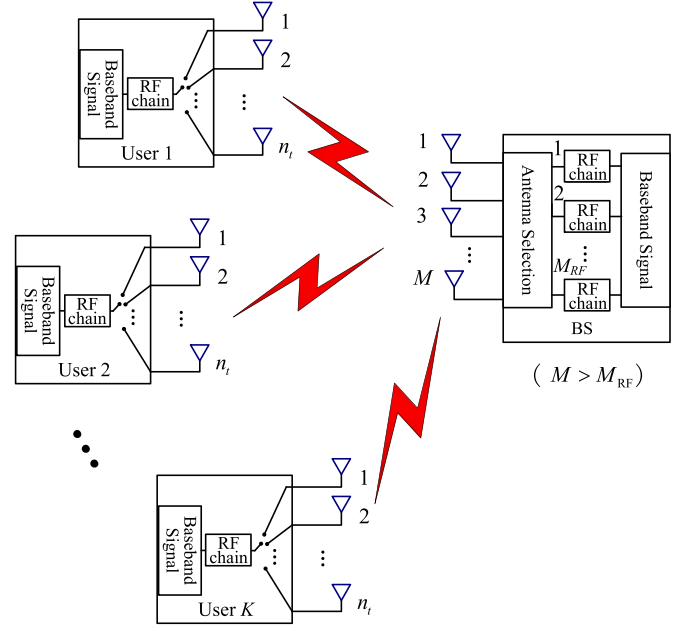


Fig. 1. In the proposed UL LS-SM-MIMO, the BS is equipped with M AEs and M_{RF} RF chains to simultaneously serve K users, where $M \gg M_{\text{RF}} > K$, and each user is equipped with $n_t > 1$ AEs and one RF chain. By exploiting the improved degree of freedom in the spatial domain, multiple users can simultaneously exploit SM for improving the UL throughput.

advantageously combining transmit precoding, receive AE selection, and channel estimation [7]–[9].

B. Uplink Multiuser Transmission

We first consider the generation of SM signals at the users. The SM signal $\mathbf{x}_k = \mathbf{e}_k s_k$ transmitted by the k th user in a time slot consists of two parts: the spatial constellation symbol $\mathbf{e}_k \in \mathbb{C}^{n_t}$ and the signal constellation symbol $s_k \in \mathbb{C}$. \mathbf{e}_k is generated by mapping $\lfloor \log_2(n_t) \rfloor$ bits to the index of the active AE, and typically, the user terminal employs $n_t = 2^p$ AEs, where p is a positive integer. Due to only a single RF chain employed at each user, only one entry of \mathbf{e}_k associated with the active AE is equal to one, and the rest of the entries of \mathbf{e}_k are zeros, i.e., we have

$$\text{supp}(\mathbf{e}_k) \in \mathbb{A}, \quad \|\mathbf{e}_k\|_0 = 1, \quad \|\mathbf{e}_k\|_2 = 1 \quad (1)$$

where $\mathbb{A} = \{1, 2, \dots, n_t\}$ is the spatial constellation symbol set. The signal constellation symbol comes from L -ary modulation, i.e., $s_k \in \mathbb{L}$, where \mathbb{L} is the signal constellation symbol set [e.g., 64 quadrature amplitude modulation (QAM)] of size L . Hence, each UL user's SM signal carries the information of $\log_2(L) + \log_2(n_t)$ bits per channel use (bpcu), and the overall UL throughput is $K(\log_2(L) + \log_2(n_t))$ bpcu. The users rely on the CPSC scheme for transmitting their SM signals [6]. Explicitly, each CPSC block consists of a cyclic prefix (CP) having the length of $P - 1$ and the associated data block having the length of Q . Hence, the length of each CPSC block is $Q + P - 1$, where this CP is capable of counteracting a dispersive multipath channel imposing dispersion over P samples. The concatenated data block consists of Q successive SM signals.

At the receiver, due to the reduced number of RF chains at the BS, only M_{RF} receive AEs can be exploited to receive signals, where existing receive AE selection schemes can be adopted to preselect M_{RF} receive AEs for achieving an improved signal detection performance [7]. Since the BS can serve K users simultaneously, after the removal of

the CP, the received signal $\mathbf{y}_q \in \mathbb{C}^{M_{\text{RF}}}$ for $1 \leq q \leq Q$ of the q th time slot of a specific CPSC block can be expressed as

$$\mathbf{y}_q = \sum_{k=1}^K \mathbf{y}_{k,q} + \mathbf{w}_q = \sum_{p=0}^{P-1} \sum_{k=1}^K \mathbf{H}_{k,p} \Theta \mathbf{x}_k \mod (q-p, Q) + \mathbf{w}_q \quad (2)$$

where $\mathbf{H}_{k,p} \in \mathbb{C}^{M \times n_t}$ is the k th user's MIMO channel matrix for the p th multipath component, i.e., $\mathbf{H}_{k,p} \Theta = \tilde{\mathbf{H}}_{k,p} \in \mathbb{C}^{M_{\text{RF}} \times n_t}$; the set Θ is determined by the AE selection scheme used; the elements of Θ having the cardinality of M_{RF} are uniquely selected from the set $\{1, 2, \dots, M\}$; \mathbf{x}_k has one nonzero entry; and $\mathbf{w}_q \in \mathbb{C}^{M_{\text{RF}}}$ is the additive white Gaussian noise (AWGN) vector with entries obeying the independent and identically distributed (i.i.d.) circularly symmetric complex Gaussian distribution with zero mean and a variance of $\sigma_w^2/2$ per dimension, which is denoted by $\mathcal{CN}(0, \sigma_w^2)$. $\mathbf{H}_{k,p} = \mathbf{R}_{\text{BS}}^{1/2} \tilde{\mathbf{H}}_{k,p} \mathbf{R}_{\text{US}}^{1/2}$, the entries of $\tilde{\mathbf{H}}_{k,p}$ obey the i.i.d. $\mathcal{CN}(0, 1)$, and \mathbf{R}_{US} with the correlation coefficient ρ_{US} and \mathbf{R}_{BS} with the correlation coefficient ρ_{BS} are correlation matrices at the users and the BS, respectively. The specific element of the m th row and the n th column of \mathbf{R}_{BS} (\mathbf{R}_{US}) is $\rho_{\text{BS}}^{|m-n|}$ ($\rho_{\text{US}}^{|m-n|}$). For correlated Rayleigh-fading MIMO channels, the specific Θ or receive AE selection scheme has an impact on the attainable system performance. In this paper, the direct AE selection scheme is used for maximizing the minimum geometric distance between any pair of the selected AEs [7]. For uniform linear arrays (ULAs), $\Theta = \{\varphi + m_{\text{RF}} \lfloor M/M_{\text{RF}} \rfloor\}_{m_{\text{RF}}=0}^{M_{\text{RF}}-1}$ with $1 \leq \varphi \leq \lfloor M/M_{\text{RF}} \rfloor - 1$. Then, (2) can be further expressed as

$$\mathbf{y}_q = \sum_{p=0}^{P-1} \tilde{\mathbf{H}}_p \mathbf{x} \mod (q-p, Q) + \mathbf{w}_q \quad (3)$$

by defining $\tilde{\mathbf{H}}_p = [\tilde{\mathbf{H}}_{1,p}, \tilde{\mathbf{H}}_{2,p}, \dots, \tilde{\mathbf{H}}_{K,p}] \in \mathbb{C}^{M_{\text{RF}} \times (n_t K)}$ and $\mathbf{x}_q = [(\mathbf{x}_{1,q})^T, (\mathbf{x}_{2,q})^T, \dots, (\mathbf{x}_{K,q})^T]^T \in \mathbb{C}^{(n_t K)}$. By considering the Q SM signals of a specific CPSC block, we arrive at

$$\mathbf{y} = \tilde{\mathbf{H}} \mathbf{x} + \mathbf{w} \quad (4)$$

where $\mathbf{y} = [(\mathbf{y}_1)^T, (\mathbf{y}_2)^T, \dots, (\mathbf{y}_Q)^T]^T \in (\mathbb{C}^{M_{\text{RF}} Q})$, the aggregate SM signal $\mathbf{x} = [(\mathbf{x}_1)^T, (\mathbf{x}_2)^T, \dots, (\mathbf{x}_Q)^T]^T \in (\mathbb{C}^{n_t K Q})$, $\mathbf{w} = [(\mathbf{w}_1)^T, (\mathbf{w}_2)^T, \dots, (\mathbf{w}_Q)^T]^T$, and

$$\tilde{\mathbf{H}} = \begin{bmatrix} \tilde{\mathbf{H}}_0 & \mathbf{0} & \mathbf{0} & \dots & \tilde{\mathbf{H}}_2 & \tilde{\mathbf{H}}_1 \\ \tilde{\mathbf{H}}_1 & \tilde{\mathbf{H}}_0 & \mathbf{0} & \dots & \vdots & \tilde{\mathbf{H}}_2 \\ \vdots & \tilde{\mathbf{H}}_1 & \tilde{\mathbf{H}}_0 & \dots & \tilde{\mathbf{H}}_{P-1} & \vdots \\ \tilde{\mathbf{H}}_{P-1} & \vdots & \tilde{\mathbf{H}}_1 & \dots & \mathbf{0} & \tilde{\mathbf{H}}_{P-1} \\ \mathbf{0} & \tilde{\mathbf{H}}_{P-1} & \vdots & \vdots & \vdots & \mathbf{0} \\ \vdots & \mathbf{0} & \tilde{\mathbf{H}}_{P-1} & \vdots & \vdots & \vdots \\ \vdots & \vdots & \mathbf{0} & \vdots & \mathbf{0} & \vdots \\ \vdots & \vdots & \vdots & \vdots & \tilde{\mathbf{H}}_0 & \mathbf{0} \\ \mathbf{0} & \mathbf{0} & \mathbf{0} & \dots & \tilde{\mathbf{H}}_1 & \tilde{\mathbf{H}}_0 \end{bmatrix} \quad (5)$$

The signal-to-noise ratio (SNR) at the receiver is defined by $\text{SNR} = E\{\|\tilde{\mathbf{H}} \mathbf{x}\|_2^2\} / E\{\|\mathbf{w}\|_2^2\}$.

The optimal signal detector for (4) relies on the ML algorithm, i.e.,

$$\begin{aligned} \min_{\hat{\mathbf{x}}} \quad & \|\mathbf{y} - \tilde{\mathbf{H}} \hat{\mathbf{x}}\|_2 = \min_{\{\hat{\mathbf{x}}_{k,q}\}_{k=1, q=1}^{K, Q}} \|\mathbf{y} - \tilde{\mathbf{H}} \hat{\mathbf{x}}\|_2 \\ \text{s.t.} \quad & \text{supp}(\hat{\mathbf{x}}_{k,q}) \in \mathbb{A}, \hat{\mathbf{x}}_{k,q} \in \mathbb{L}, 1 \leq k \leq K, 1 \leq q \leq Q \end{aligned} \quad (6)$$

whose complexity exponentially increases with the number of users since the size of the search set for the ML detector is $(n_t \cdot L)^{KQ}$. This excessive complexity can be unaffordable in practice. To reduce the complexity, near-optimal sphere decoding detectors have been proposed [10], but their complexity may still remain high, particularly for the systems supporting large K , Q , n_t , and L [11]. In conventional LS-MIMO systems, low-complexity linear signal detectors (e.g., the MMSE-based signal detector) have been shown to be near optimal since $M = M_{\text{RF}} \gg K$ and $n_t = 1$ make multiuser signal detection an *overdetermined* problem [4]. However, in the proposed scheme, we have $M_{\text{RF}} < K n_t$. Hence, the multiuser signal detection problem (6) represents a large-scale *underdetermined* problem. Consequently, the conventional linear signal detectors perform poorly in the proposed LS-SM-MIMO [11]. By exploiting the sparsity of SM signals, the authors in [11]–[13] have proposed the concept of CS-based signal detectors for the downlink of small-scale SM-MIMO operating in a single-user scenario. However, these signal detectors are unsuitable for the proposed multiuser scenarios. Observe from (1) that $\mathbf{x}_{k,q}$ is a sparse signal having a sparsity level of one. Hence, the aggregate SM signal \mathbf{x} , which consists of multiple users' SM signals in Q time slots, exhibits distributed sparsity with the sparsity level of KQ . This property of \mathbf{x} inspires us to exploit the SCS theory for the multiuser signal detection [14]. To further improve the signal detection performance and to increase the system's throughput, we propose a joint SM transmission scheme and an SCS-based MUD, which will be detailed in the following section.

III. SCS-BASED MUD FOR LS-SM-MIMO UL

To solve the multiuser signal detection of our UL LS-SM-MIMO system, we first propose a joint SM transmission scheme to be employed at the users. Accordingly, an SCS-based low-complexity MUD is developed at the BS, whereby the distributed sparsity of the aggregate SM signal and the group sparsity of multiple aggregate SM signals are exploited. Moreover, the computational complexity of the proposed SCS-based MUD is discussed.

A. Joint SM Transmission Scheme at the Users

For the k th user in the q th time slot, every successive J CPSC block is considered as a group, and they share the same spatial constellation symbol, i.e.,

$$\text{supp}(\mathbf{x}_{k,q}^{(1)}) = \text{supp}(\mathbf{x}_{k,q}^{(2)}) = \dots = \text{supp}(\mathbf{x}_{k,q}^{(J)}), \quad 1 \leq k \leq K, 1 \leq q \leq Q \quad (7)$$

where we introduce the superscript (j) to denote the j th CPSC block and J is typically small, e.g., $J = 2$. In CS theory, the specific signal structure, where $\mathbf{x}_{k,q}^{(1)}, \mathbf{x}_{k,q}^{(2)}, \dots, \mathbf{x}_{k,q}^{(J)}$ share a common support, is often referred to as the *group sparsity*. Similarly, the aggregate SM signals consisting of the K users' SM signals also exhibit group sparsity, i.e.,

$$\text{supp}(\mathbf{x}^{(1)}) = \text{supp}(\mathbf{x}^{(2)}) = \dots = \text{supp}(\mathbf{x}^{(J)}). \quad (8)$$

Although exhibiting group sparsity may slightly reduce the information carried by the spatial constellation symbols, it is also capable of

reducing the number of the RF chains required according to the SCS theory, while simultaneously improving the total bit error rate (BER) of the entire system even with higher UL throughput. This conclusion will be confirmed by our simulation results.

B. SCS-Based MUD at the BS

According to (4), the received signals at the BS in the same group can be expressed as

$$\mathbf{y}^{(j)} = \tilde{\mathbf{H}}^{(j)} \mathbf{x}^{(j)} + \mathbf{w}^{(j)}, \quad 1 \leq j \leq J \quad (9)$$

where $\mathbf{y}^{(j)}$ denotes the received signal in the j th CPSC block, whereas $\tilde{\mathbf{H}}^{(j)}$ and $\mathbf{w}^{(j)}$ are the effective MIMO channel matrix and the AWGN vector, respectively.

The intrinsically distributed sparsity of $\mathbf{x}^{(j)}$ and the underdetermined nature of (9) inspire us to solve the signal detection problem based on CS theory, which can efficiently acquire the sparse solutions to underdetermined linear systems. Moreover, the J different aggregate SM signals in (9) can be jointly exploited for improving the signal detection performance due to the group sparsity of $\{\mathbf{x}^{(j)}\}_{j=1}^J$. Thus, by considering both the distributed sparsity and the group sparsity of the aggregate SM signals, the multiuser signal detection at the BS can be formulated as the following optimization problem:

$$\begin{aligned} \min_{\{\hat{\mathbf{x}}^{(j)}\}_{j=1}^J} \quad & \sum_{j=1}^J \|\mathbf{y}^{(j)} - \tilde{\mathbf{H}}^{(j)} \hat{\mathbf{x}}^{(j)}\|_2^2 = \min_{\{\hat{\mathbf{x}}_{k,q}^{(j)}\}_{j=1, k=1, q=1}^{J, K, Q}} \\ \text{s.t.} \quad & \sum_{j=1}^J \|\mathbf{y}^{(j)} - \tilde{\mathbf{H}}^{(j)} \hat{\mathbf{x}}^{(j)}\|_2^2 \\ & \|\hat{\mathbf{x}}_{k,q}^{(j)}\|_0 = 1, \quad 1 \leq j \leq J, \quad 1 \leq q \leq Q, \quad 1 \leq k \leq K. \end{aligned} \quad (10)$$

Our proposed SCS-based MUD solves the optimization problem (10) with the aid of two steps. In the first step, we estimate the spatial constellation symbols, i.e., the indexes of K users' active AEs in J successive CPSC blocks. In the second step, we infer the legitimate signal constellation symbols of the K users in J CPSC blocks.

1. Step 1—Estimation of Spatial Constellation Symbols: We propose a group subspace pursuit (GSP) algorithm developed from the classical subspace pursuit (SP) algorithm in [15] to acquire the sparse solution to the large-scale underdetermined problem (10), where both the *a priori* sparse information (i.e., $\|\mathbf{x}_{k,q}^{(j)}\|_0 = 1$) and the group sparsity of $\mathbf{x}^{(1)}, \mathbf{x}^{(2)}, \dots, \mathbf{x}^{(J)}$ are exploited for improving the multiuser signal detection performance. The proposed GSP algorithm is described in **Algorithm 1**, which estimates SM signal $\{\hat{\mathbf{x}}_{k,q}^{(j)}\}_{k=1, j=1, q=1}^{K, J, Q}$. Hence, the estimated spatial constellation symbol is $\{\text{supp}(\hat{\mathbf{x}}_{k,q}^{(j)})\}_{k=1, j=1, q=1}^{K, J, Q}$.

Algorithm 1 Proposed GSP Algorithm.

Input: Noisy received signals $\mathbf{y}^{(j)}$ and effective channel matrices $\tilde{\mathbf{H}}^{(j)}$ for $1 \leq j \leq J$.
Output: Estimated $\hat{\mathbf{x}}^{(j)} = [(\hat{\mathbf{x}}_1^{(j)})^T, (\hat{\mathbf{x}}_2^{(j)})^T, \dots, (\hat{\mathbf{x}}_Q^{(j)})^T]^T$, where $\hat{\mathbf{x}}_q^{(j)} = [(\hat{\mathbf{x}}_{1,q}^{(j)})^T, (\hat{\mathbf{x}}_{2,q}^{(j)})^T, \dots, (\hat{\mathbf{x}}_{K,q}^{(j)})^T]^T$ for $1 \leq q \leq Q$.
1: $\mathbf{r}^{(j)} = \mathbf{y}^{(j)}$ for $1 \leq j \leq J$; {Initialization}
2: $\Omega^0 = \emptyset$; {Empty support set}
3: $t = 1$; {Iteration index}

4: repeat
5: $\mathbf{a}_{k,q}^{(j)} = (\tilde{\mathbf{H}}_{k,q}^{(j)})^* \mathbf{r}^{(j)}$ for $1 \leq k \leq K$, $1 \leq q \leq Q$, and $1 \leq j \leq J$; {Correlation}
6: $\tau_{k,q} = \arg \max_{\tau_{k,q}} \sum_{j=1}^J \|\mathbf{a}_{k,q}^{(j)}\|_{\tau_{k,q}}^2$ for $1 \leq k \leq K$, $1 \leq q \leq Q$; {Identify support}
7: $\Gamma = \{\tau_{k,q} + (k-1 + K(q-1))n_t\}_{k=1, q=1}^{K, Q}$; {Preliminary support set}
8: $\mathbf{b}^{(j)}|_{\Omega^{t-1} \cup \Gamma} = (\tilde{\mathbf{H}}^{(j)}|_{\Omega^{t-1} \cup \Gamma})^\dagger \mathbf{y}^{(j)}$ for $1 \leq j \leq J$; {Least squares}
9: $\omega_{k,q} = \arg \max_{\omega_{k,q}} \sum_{j=1}^J \|\mathbf{b}_{k,q}^{(j)}\|_{\omega_{k,q}}^2$ for $1 \leq k \leq K$, $1 \leq q \leq Q$; {Pruning support set}
10: $\Omega^t = \{\omega_{k,q} + (k-1 + K(q-1))n_t\}_{k=1, q=1}^{K, Q}$; {Final support set}
11: $\mathbf{c}^{(j)}|_{\Omega^t} = (\tilde{\mathbf{H}}^{(j)}|_{\Omega^t})^\dagger \mathbf{y}^{(j)}$ for $1 \leq j \leq J$; {Least squares}
12: $\mathbf{r}^{(j)} = \mathbf{y}^{(j)} - \tilde{\mathbf{H}}^{(j)} \mathbf{c}^{(j)}$ for $1 \leq j \leq J$; {Compute residual}
13: $t = t + 1$; {Update iteration index}
14: until $\Omega^t = \Omega^{t-1}$ or $t \geq Q$

Compared with the classical SP algorithm, the proposed GSP algorithm exploits the distributed sparsity and group sparsity of $\{\mathbf{x}^{(j)}\}_{j=1}^J$. More explicitly, $\mathbf{x}^{(j)} \in \mathbb{C}^{(KQn_t)}$ consists of the KQ low-dimensional sparse vectors $\mathbf{x}_{k,q}^{(j)} \in \mathbb{C}^{n_t}$, where each $\mathbf{x}_{k,q}^{(j)}$ has the known sparsity level of one, and the aggregate SM signals $\mathbf{x}^{(1)}, \mathbf{x}^{(2)}, \dots, \mathbf{x}^{(J)}$ exhibit group sparsity. Specifically, the differences between the proposed GSP algorithm and the classical SP algorithm lie in the following two aspects: 1) the identification of the support set including the steps of the *preliminary support set* and the *final support set* as shown in **Algorithm 1**; and 2) the joint processing of $\mathbf{y}^{(1)}, \mathbf{y}^{(2)}, \dots, \mathbf{y}^{(J)}$. First, for the support selection, taking the step of the *preliminary support set* for instance, when selecting the preliminary support set, the classical SP algorithm selects the support set associated with the first KQ largest values of the global correlation result $(\tilde{\mathbf{H}}^{(j)})^* \mathbf{r}^{(j)}$. By contrast, the proposed GSP algorithm selects the support set associated with the largest value from the local correlation result in each $(\tilde{\mathbf{H}}_{k,q}^{(j)})^* \mathbf{r}^{(j)}$. This way, the distributed sparsity of the aggregate SM signal can be exploited for improved signal detection performance. Second, compared with the classical SP algorithm, the proposed GSP algorithm jointly exploits the J correlated signals having the group sparsity, which can bring the further improved signal detection performance.

It should be noted that even for the special case of $J = 1$, i.e., without using the joint SM transmission scheme, the proposed GSP algorithm still achieves a better signal detection performance than the classical SP algorithm when handling the aggregate SM signal, since the inherently distributed sparsity of the aggregate SM signal is leveraged to improve the signal detection performance.

2. Step 2—Acquisition of Signal Constellation Symbols: Following *Step 1*, we can also acquire a rough estimate of the signal constellation symbol for each user in each time slot. By searching for the minimum Euclidean distance between this rough estimate of the signal constellation symbol and the legitimate constellation symbols of \mathbb{L} , we can obtain the final estimate of signal constellation symbols.

C. Computational Complexity

The optimal ML signal detector has a prohibitively high computational complexity of $\mathcal{O}((L \cdot n_t)^{(K \cdot Q)})$ according to (6). The sphere decoding detectors [10] are indeed capable of reducing the computational complexity, but they may still suffer from unaffordable complexity, particularly for large K , Q , L , and n_t values. By contrast, the conventional MMSE-based detector for LS-MIMO and CS-based

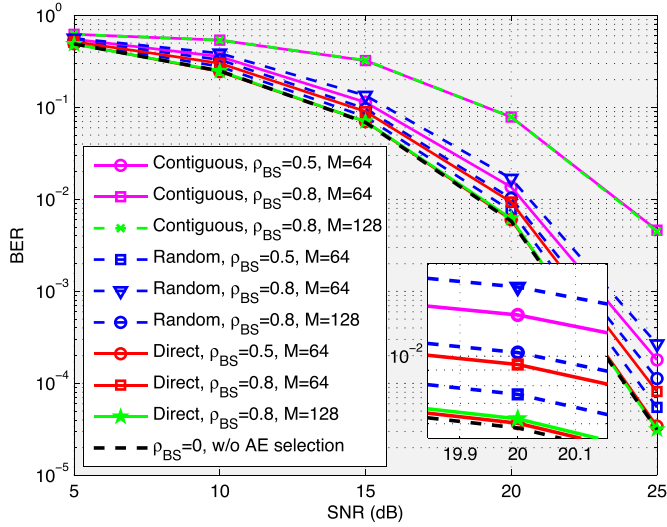


Fig. 2. Total BERs achieved by the proposed SCS-based MUD with different AE selection schemes, where $K = 8$, $J = 2$, 64-QAM, $M_{\text{RF}} = 18$, $n_t = 4$, and $\rho_{\text{US}} = 0$ are considered.

361 detector [13] for small-scale SM-MIMO enjoy the low complexity of
 362 $\mathcal{O}(M_{\text{RF}} \cdot (n_t \cdot Q \cdot K)^2 + (n_t \cdot Q \cdot K)^3)$ and $\mathcal{O}(2M_{\text{RF}} \cdot (Q \cdot K)^2 +$
 363 $(Q \cdot K)^3)$, respectively. For the proposed SCS-based MUD, most
 364 of the computational requirements are imposed by the least squares
 365 (LS) operations, which has complexity of $\mathcal{O}(J \cdot (2M_{\text{RF}} \cdot (Q \cdot K)^2 +$
 366 $(Q \cdot K)^3))$ [16]. Consequently, the computational complexity per
 367 CPSC block is $\mathcal{O}(2M_{\text{RF}} \cdot (Q \cdot K)^2 + (Q \cdot K)^3)$, since J successive
 368 aggregate SM signals are jointly processed. Compared with conven-
 369 tional signal detectors, the proposed SCS-based MUD benefits from
 370 substantially lower complexity, and it has similar low complexity as
 371 the conventional MMSE- and CS-based signal detectors.

IV. SIMULATION RESULTS

373 A simulation study was carried out to compare the attainable perfor-
 374 mance of the proposed SCS-based MUD to that of the MMSE-based
 375 signal detector [4] and to that of the CS-based signal detector [13].
 376 In the LS-SM-MIMO system considered, the BS used a ULA relying
 377 on a large number of AEs M , but a much smaller number of RF
 378 chains M_{RF} , whereas K users employing n_t AEs but only a single RF
 379 chain simultaneously use the CPSC scheme associated with $P = 8$ and
 380 $Q = 64$ to transmit the SM signals to the BS. The total BER including
 381 both the spatial constellation symbols and the signal constellation
 382 symbols was evaluated.

383 Fig. 2 compares the total BERs achieved by the proposed SCS-based
 384 MUD with different AE selection schemes, where $K = 8$, $J = 2$,
 385 64-QAM, $M_{\text{RF}} = 18$, $n_t = 4$, and $\rho_{\text{US}} = 0$ are considered. The con-
 386 tiguous AE selection scheme implies that we select M_{RF} adjacent
 387 AEs, i.e., $\Theta = \{\varphi + m_{\text{RF}}\}_{m_{\text{RF}}=0}^{M_{\text{RF}}-1}$ with $1 \leq \varphi \leq M - M_{\text{RF}} + 1$. By
 388 contrast, in the random AE selection scheme, the elements of Θ are
 389 randomly selected from the set $\{1, 2, \dots, M\}$, whereas the direct
 390 AE selection scheme in [7] has been described in Section II-B.
 391 Furthermore, the BER achieved by the SCS-based MUD relying on
 392 $\rho_{\text{BS}} = 0$ is also considered as a performance bound, since the choice
 393 of $\rho_{\text{BS}} = 0$ and $\rho_{\text{US}} = 0$ implies the uncorrelated Rayleigh-fading
 394 MIMO channels. Observe from Fig. 2 that the direct AE selection
 395 scheme outperforms the other pair of AE selection schemes. Moreover,
 396 for a certain AE selection scheme, the BER performance degrades
 397 when M_{RF}/M or ρ_{BS} increases. For the direct AE selection scheme,
 398 the BER performance of $\rho_{\text{BS}} = 0.8$, $M = 128$ and of $\rho_{\text{BS}} = 0.5$,

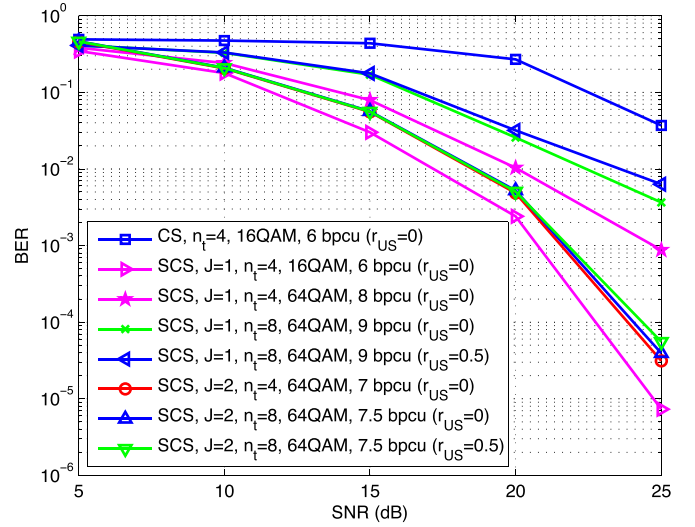


Fig. 3. Total BERs achieved by the CS-based signal detector and the SCS-based MUD against different SNRs in LS-SM-MIMO, where $K = 8$, $M_{\text{RF}} = 18$, $M = 64$, $\rho_{\text{BS}} = 0.5$, and the direct AE selection scheme is considered.

$M = 64$ approaches the BER achieved for transmission over uncor- 399
 related Rayleigh-fading MIMO channels, which confirms the near- 400
 optimal performance of the direct AE selection scheme. 401

Fig. 3 compares the overall BER achieved by the CS-based signal 402
 detector and by the proposed SCS-based MUD versus the SNR in our 403
 LS-SM-MIMO context, where $K = 8$, $M_{\text{RF}} = 18$, $M = 64$, $\rho_{\text{BS}} = 0.5$, 404
 and the direct AE selection scheme is considered. The SCS-based 405
 MUD outperforms the CS-based signal detector even for $J = 1$, since 406
 the distributed sparsity of the aggregate SM signal is exploited. For the 407
 SCS-based MUD, the BER performance improves when J increases, 408
 albeit this is achieved at the cost of reduced UL throughput. To mitigate 409
 this impediment, a higher number of AEs can be employed by the users 410
 for expanding the spatial constellation symbol set constituted by the 411
 AEs. Specifically, by increasing n_t from 4 to 8, the UL throughput 412
 of the SCS-based MUD may be increased, but having more AEs at 413
 the user results in a higher ρ_{US} . When n_t is increased, the BER 414
 performance of the SCS-based MUD associated with $J = 1$ degrades, 415
 as expected. By contrast, when n_t is increased, the BER performance 416
 loss of the SCS-based MUD using $J = 2$ can be less than 0.2 dB if the 417
 BER of 10^{-4} is considered, even when a higher ρ_{US} associated with a 418
 higher n_t is considered. 419

Fig. 4 portrays the BER achieved by the different signal detectors as 420
 a function of the SNR in the context of the proposed LS-SM-MIMO 421
 for $K = 8$, $M_{\text{RF}} = 18$, $M = 64$, $n_t = 4$, $\rho_{\text{BS}} = 0.5$, and $\rho_{\text{US}} = 0$, 422
 where the direct AE selection scheme is also considered. In Fig. 4, 423
 we also characterize the ‘oracle-assisted’ LS-based signal detector 424
 relying on the assumption that the spatial constellation symbol is 425
 perfectly known at the BS for the proposed LS-SM-MIMO scheme 426
 associated with $J = 2$, 64-QAM as well as for the MMSE-based 427
 LS-MIMO detector in conjunction with 64-QAM, where both of them 428
 only consider the BER of the classic signal constellation symbol. Here, 429
 we assume that the LS-MIMO arrangement uses the same number 430
 of RF chains to serve eight single-antenna users communicating 431
 over uncorrelated Rayleigh-fading channels. The superiority of our 432
 SCS-based MUD over the MMSE- and CS-based signal detectors 433
 becomes clear. 434

Moreover, the performance gap between the oracle LS-based signal 435
 detector associated with 7 bpcu and the proposed SCS-based MUD 436
 with 7 bpcu is less than 0.5 dB. Note again that the oracle LS-based sig- 437
 nal detector only considers the BER of the classic signal constellation 438

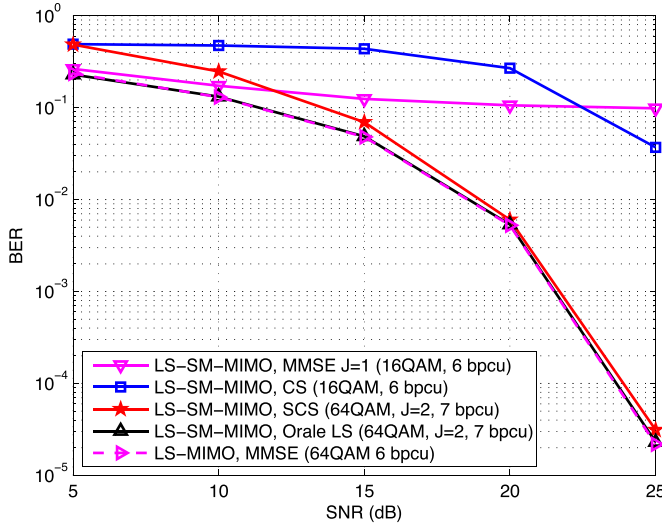


Fig. 4. Total BERs achieved by different signal detectors against different SNRs in the proposed LS-SM-MIMO and conventional LS-MIMO.

symbol, whereas the proposed SCS-based MUD considers both the spatial and the classic signal constellation symbols. Finally, compared with the conventional LS-MIMO using the MMSE-based signal detector (6 bpcu), our proposed UL LS-SM-MIMO and the associated SCS-based MUD (7 bpcu) only suffer from a negligible BER loss, which explicitly confirmed the improved UL throughput of the proposed LS-SM-MIMO scheme.

V. CONCLUSION

We have proposed an LS-SM-MIMO scheme for the UL transmission. The BS employs a large number of AEs but a much smaller number of RF chains, where a simple receive AE selection scheme is used for the improved performance. Each user equipped with multiple AEs but only a single RF chain uses CPSC to combat multipath channels. SM has been adopted for the UL transmission to improve the UL throughput. The proposed scheme is particularly suitable for scenarios where a large number of low-cost AEs can be accommodated, and both power consumption and hardware cost are heavily determined by the number of RF chains. Due to the reduced number of RF chains at the BS and multiple AEs employed by each user, the UL multiuser signal detection is a challenging large-scale underdetermined problem. We have proposed a joint SM transmission scheme at the users to introduce the group sparsity of multiple aggregate SM signals, and a

matching SCS-based MUD at the BS has been proposed to leverage the inherently distributed sparsity of the aggregate SM signal as well as the group sparsity of multiple aggregate SM signals for reliable multiuser signal detection performance. The proposed SCS-based MUD enjoys the low complexity, and our simulation results have demonstrated that it performs better than its conventional counterparts with even much higher UL throughput.

REFERENCES

- [1] M. D. Renzo, H. Haas, A. Ghayeb, S. Sugiura, and L. Hanzo, "Spatial modulation for generalized MIMO: Challenges, opportunities and implementation," *Proc. IEEE*, vol. 102, no. 1, pp. 56–103, Jan. 2014.
- [2] A. Younis, R. Mesleh, M. Di Renzo, and H. Haas, "Generalised spatial modulation for large-scale MIMO," in *Proc. EUSIPCO*, Sep. 2014, pp. 346–350.
- [3] S. Ganesan, R. Mesleh, H. Haas, C. Ahn, and S. Yun, "On the performance of spatial modulation OFDM," in *Proc. 40th Asilomar Conf. Signals, Syst. Comput.*, Oct. 2006, pp. 1825–1829.
- [4] F. Rusek *et al.*, "Scaling up MIMO: Opportunities and challenges with very large arrays," *IEEE Signal Process. Mag.*, vol. 30, no. 1, pp. 40–60, Jan. 2013.
- [5] N. Serafimovski *et al.*, "Practical implementation of spatial modulation," *IEEE Trans. Veh. Technol.*, vol. 62, no. 9, pp. 4511–4523, Nov. 2013.
- [6] P. Som and A. Chockalingam, "Spatial modulation and space shift keying in single carrier" in *Proc. IEEE Int. Symp. PIMRC*, Sep. 2012, pp. 1062–1067.
- [7] X. Wu, M. Di Renzo, and H. Haas, "Adaptive selection of antennas for optimum transmission in spatial modulation," *IEEE Trans. Wireless Commun.*, vol. 14, no. 7, pp. 3630–3641, Jul. 2015.
- [8] S. Narayanan *et al.*, "Multi-user spatial modulation MIMO" in *Proc. IEEE WCNC*, Apr. 2014, pp. 671–676.
- [9] X. Wu, H. Claussen, M. D. Renzo, and H. Haas, "Channel estimation for spatial modulation," *IEEE Trans. Commun.*, vol. 62, no. 12, pp. 4362–4372, Dec. 2014.
- [10] A. Younis, S. Sinanovic, M. Di Renzo, R. Mesleh, and H. Haas, "Generalised sphere decoding for spatial modulation," *IEEE Trans. Commun.*, vol. 61, no. 7, pp. 2805–2815, Jul. 2013.
- [11] W. Liu, N. Wang, M. Jin, and H. Xu, "Denoising detection for the generalized spatial modulation system using sparse property," *IEEE Commun. Lett.*, vol. 18, no. 1, pp. 22–25, Jan. 2014.
- [12] B. Shim, S. Kwon, and B. Song, "Sparse detection with integer constraint using multipath matching pursuit," *IEEE Commun. Lett.*, vol. 18, no. 10, pp. 1851–1854, Oct. 2014.
- [13] C. Yu *et al.*, "Compressed sensing detector design for space shift keying in MIMO systems," *IEEE Commun. Lett.*, vol. 16, no. 10, pp. 1556–1559, Oct. 2012.
- [14] M. F. Duarte and Y. C. Eldar, "Structured compressed sensing: From theory to applications," *IEEE Trans. Signal Process.*, vol. 59, no. 9, pp. 4053–4085, Sep. 2011.
- [15] W. Dai and O. Milenkovic, "Subspace pursuit for compressive sensing signal reconstruction," *IEEE Trans. Inf. Theory*, vol. 55, no. 5, pp. 2230–2249, May 2009.
- [16] A. Björck, *Numerical Methods for Matrix Computations*. Cham, Switzerland: Springer Int. Publ. AG, 2014.

AUTHOR QUERY

NO QUERY.

Correspondence

Compressive-Sensing-Based Multiuser Detector for the Large-Scale SM-MIMO Uplink

Zhen Gao, Linglong Dai, Zhaocheng Wang, *Senior Member, IEEE*,
Sheng Chen, *Fellow, IEEE*, and Lajos Hanzo, *Fellow, IEEE*

Abstract—Conventional spatial modulation (SM) is typically considered for transmission in the downlink of small-scale multiple-input-multiple-output (MIMO) systems, where a single antenna element (AE) of a set of, e.g., 2^P AEs is activated for implicitly conveying p bits. By contrast, inspired by the compelling benefits of large-scale MIMO (LS-MIMO) systems, here, we propose an LS-SM-MIMO scheme for the uplink (UL), where each user having multiple AEs but only a single radio frequency (RF) chain invokes SM for increasing the UL throughput. At the same time, by relying on hundreds of AEs and a small number of RF chains, the base station (BS) can simultaneously serve multiple users while reducing the power consumption. Due to the large number of AEs of the UL users and the comparably small number of RF chains at the BS, the UL multiuser signal detection becomes a challenging large-scale underdetermined problem. To solve this problem, we propose a joint SM transmission scheme and a carefully designed structured compressive sensing (SCS)-based multiuser detector (MUD) to be used at the users and the BS, respectively. Additionally, the cyclic-prefix single carrier (CPSC) is used to combat the multipath channels, and a simple receive AE selection is used for the improved performance over correlated Rayleigh-fading MIMO channels. We demonstrate that the aggregate SM signal consisting of multiple UL users' SM signals of a CPSC block exhibits distributed sparsity. Moreover, due to the joint SM transmission scheme, aggregate SM signals in the same transmission group exhibit group sparsity. By exploiting these intrinsically sparse features, the proposed SCS-based MUD can reliably detect the resultant SM signals with low complexity. Simulation results demonstrate that the proposed SCS-based MUD achieves a better signal detection performance than its counterparts even with higher UL throughput.

Index Terms—Compressive sensing (CS), large-scale multiple-input-multiple-output (LS-MIMO), multiuser detector (MUD), spatial modulation (SM).

I. INTRODUCTION

A widely recognized consensus is that fifth-generation (5G) systems will be capable of providing significant energy efficiency and system capacity improvements [1], [2]. Promising techniques, such as large-scale multiple-input-multiple-output (LS-MIMO) and spatial modulation (SM)-MIMO systems, are considered as potent candidates for 5G systems [1]–[5]. LS-MIMO employing hundreds of antenna

elements (AEs) at the base station (BS) is capable of improving spectral efficiency by orders of magnitude, but it suffers from the nonnegligible power consumption and hardware cost due to one specific radio frequency (RF) chain usually required by every AE [5]. By using a reduced number of RF chains, the emerging SM-MIMO activates part of available AEs to transmit extra information in the spatial domain, and it has attracted much attention due to its high energy efficiency and reduced hardware cost [5]. However, conventional SM-MIMO is usually considered in the downlink of small-scale MIMO systems, and therefore, its achievable capacity is limited. Individually, both technologies have their own advantages and drawbacks. By an effective combination of them, one can envision the win-win situation. SM-MIMO is attractive for LS-MIMO systems, since the reduced number of required RF chains in SM-MIMO can reduce the power consumption and hardware cost in conventional LS-MIMO systems. Moreover, hundreds of AEs used in LS-MIMO can improve the system throughput of SM-MIMO. Such reciprocity enables LS-MIMO and SM-MIMO to enjoy the apparent compatibility.

In this paper, we propose an LS-SM-MIMO scheme for intrinsically amalgamating the compelling benefits of both LS-MIMO and SM-MIMO for the 5G uplink (UL) over frequency-selective fading channels. In the proposed scheme, each UL user equipped with multiple AEs but only a single RF chain invokes SM for increasing the UL throughput, and the cyclic-prefix single-carrier (CPSC) transmission scheme is adopted to combat the multipath channels [6]. At the BS, hundreds of AEs but only dozens of RF chains are employed to simultaneously serve multiple users, and a direct AE selection scheme is used to improve the system performance over correlated Rayleigh-fading MIMO channels at the BS [7]. The proposed scheme can be adopted in conventional LS-MIMO as a specific UL-transmission mode for reducing the power consumption or, alternatively, for energy- and cost-efficient LS-SM-MIMO, where joint benefits of efficient AE selection [7], transmit precoding [8], and channel estimation [9] can be readily exploited. To sum up, the proposed scheme inherits the advantages of LS-MIMO and SM-MIMO, while reducing the power consumption and hardware cost.

A challenging problem in the proposed UL LS-SM-MIMO scheme is how to realize a reliable multiuser detector (MUD) with low complexity. The optimal maximum likelihood (ML) signal detector suffers from excessive complexity. Conventional sphere decoding detectors cannot be readily used in multiuser scenarios and may still exhibit high complexity for LS-SM-MIMO [10]. Existing low-complexity linear signal detectors, e.g., the minimum mean square error (MMSE)-based signal detector, perform well for conventional LS-MIMO systems [4]. However, they are unsuitable for the proposed LS-SM-MIMO UL transmission, since the large number of transmit AEs of the UL users and the reduced number of receive RF chains at the BS make UL multiuser signal detection a large-scale underdetermined/rank-deficient problem. The authors in [11]–[13] proposed compressive sensing (CS)-based signal detectors to solve the underdetermined signal detection problem in SM-MIMO systems, but they only considered the single-user small-scale SM-MIMO systems in the downlink.

Against this background, our new contribution is that we exploit the specific signal structure in the proposed multiuser LS-SM-MIMO UL transmission, where each user only activates a single AE in each time slot. Hence, the SM signal of each UL user is sparse with

Manuscript received May 7, 2015; revised October 1, 2015; accepted November 14, 2015. This work was supported in part by the International Science and Technology Cooperation Program of China under Grant 2015DFG12760, by the National Natural Science Foundation of China under Grant 61571270 and Grant 61201185, by the Beijing Natural Science Foundation under Grant 4142027, and by the Foundation of Shenzhen government. The review of this paper was coordinated by Dr. Y. Xin.

Z. Gao, L. Dai, and Z. Wang are with the Tsinghua National Laboratory for Information Science and Technology (TNList), Department of Electronic Engineering, Tsinghua University, Beijing 100084, China (e-mail: gao-z11@mails.tsinghua.edu.cn; daill@mail.tsinghua.edu.cn; zcwang@mail.tsinghua.edu.cn).

S. Chen and L. Hanzo are with the School of Electronics and Computer Science, University of Southampton, Southampton SO17 1BJ, U.K. (e-mail: sqc@ecs.soton.ac.uk; lh@ecs.soton.ac.uk).

Color versions of one or more of the figures in this paper are available online at <http://ieeexplore.ieee.org>.

Digital Object Identifier 10.1109/TVT.2015.2501460

the sparsity level of one, and the aggregate SM signal consisting of multiple UL users' SM signals of a CPSC block exhibits certain distributed sparsity, which can be beneficially exploited for improving the signal detection performance at the BS. Moreover, we propose a joint SM transmission scheme for the UL users in conjunction with an appropriately structured CS (SCS)-based MUD at the BS. The proposed SCS-based MUD is specifically tailored to leverage the inherently distributed sparsity of the aggregate SM signal and the group sparsity of multiple aggregate SM signals, owing to the joint SM transmission scheme for reliable signal detection performance. Our simulation results demonstrate that the proposed SCS-based MUD is capable of outperforming the conventional detectors even with higher UL throughput.

The rest of this paper is organized as follows. Section II introduces the system model of the proposed LS-SM-MIMO scheme. Section III specifies the proposed joint SM transmission and SCS-based MUD. Section IV provides our simulation results. Section V concludes this paper.

Throughout this paper, lowercase and uppercase boldface letters denote vectors and matrices, respectively, whereas $(\cdot)^T$, $(\cdot)^*$, $(\cdot)^\dagger$, and $[\cdot]$ denote the transpose, conjugate transpose, Moore–Penrose matrix inversion, and the integer floor operators, respectively. The l_0 and l_2 norm operations are given by $\|\cdot\|_0$ and $\|\cdot\|_2$, respectively. The support set of vector \mathbf{x} is denoted by $\text{supp}\{\mathbf{x}\}$, and \mathbf{x}_i denotes the i th entry of vector \mathbf{x} . Additionally, $\mathbf{x}|_\Gamma$ denotes the entries of \mathbf{x} defined in the set Γ , $\Phi|_\Gamma$ denotes the submatrix whose columns comprise the columns of Φ that are defined in Γ , and $\Phi|_\Gamma$ denotes the submatrix whose rows comprise the rows of Φ that are defined in Γ . The expectation operator is given by $E\{\cdot\}$. $\text{mod}(x, y) = x - \lfloor x/y \rfloor y$ if $y \neq 0$ and $x - \lfloor x/y \rfloor y \neq 0$, whereas $\text{mod}(x, y) = y$ if $y \neq 0$ and $x - \lfloor x/y \rfloor y = 0$.

II. SYSTEM MODEL

We first introduce the proposed LS-SM-MIMO scheme and then focus our attention on the UL transmission with an emphasis on the multiuser signal detection.

A. Proposed Multiuser LS-SM-MIMO Scheme

As shown in Fig. 1, we consider the proposed LS-SM-MIMO from both the BS side and the user side. For conventional LS-MIMO, the number of AEs employed by the BS is equal to the number of its RF chains [4]. However, the BS in LS-SM-MIMO, as shown in Fig. 1, is equipped with a much smaller number of RF chains M_{RF} than the total number of AEs M , i.e., we have $M_{\text{RF}} \ll M$. Conventional LS-MIMO systems typically assume single-antenna users [4]. By contrast, in the proposed scheme, each user is equipped with $n_t > 1$ AEs but only a single RF chain, and SM is adopted for the UL transmission, where only one of the available AEs is activated for data transmission. It has been shown that the main power consumption and hardware cost of cellular networks comes from the radio access network [1]. Hence, using a reduced number of expensive RF chains compared with the total number of AEs at the BS can substantially reduce both the power consumption and the hardware cost for the operators. Meanwhile, it is feasible to incorporate several AEs and a single RF chain in the handsets. The resultant increased degrees of freedom in the spatial domain may then be exploited for improving the UL throughput. The proposed scheme can be considered as an optional UL-transmission mode in conventional LS-MIMO systems, where AE selection schemes may be adopted for beneficially selecting the most suitable M_{RF} AEs at the BS to receive UL SM signals [7]. Alternatively, it can also be used for the UL of LS-SM-MIMO, when

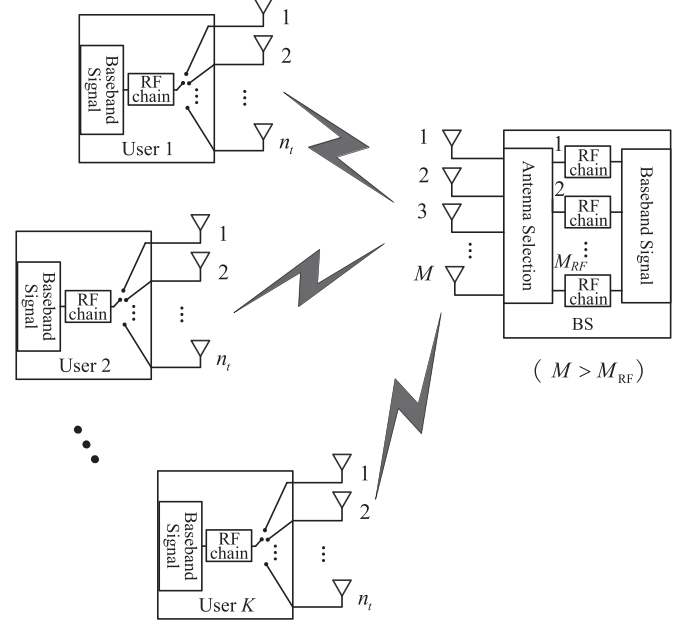


Fig. 1. In the proposed UL LS-SM-MIMO, the BS is equipped with M AEs and M_{RF} RF chains to simultaneously serve K users, where $M \gg M_{\text{RF}} > K$, and each user is equipped with $n_t > 1$ AEs and one RF chain. By exploiting the improved degree of freedom in the spatial domain, multiple users can simultaneously exploit SM for improving the UL throughput.

advantageously combining transmit precoding, receive AE selection, and channel estimation [7]–[9].

B. Uplink Multiuser Transmission

We first consider the generation of SM signals at the users. The SM signal $\mathbf{x}_k = \mathbf{e}_k s_k$ transmitted by the k th user in a time slot consists of two parts: the spatial constellation symbol $\mathbf{e}_k \in \mathbb{C}^{n_t}$ and the signal constellation symbol $s_k \in \mathbb{C}$. \mathbf{e}_k is generated by mapping $\lfloor \log_2(n_t) \rfloor$ bits to the index of the active AE, and typically, the user terminal employs $n_t = 2^p$ AEs, where p is a positive integer. Due to only a single RF chain employed at each user, only one entry of \mathbf{e}_k associated with the active AE is equal to one, and the rest of the entries of \mathbf{e}_k are zeros, i.e., we have

$$\text{supp}(\mathbf{e}_k) \in \mathbb{A}, \quad \|\mathbf{e}_k\|_0 = 1, \quad \|\mathbf{e}_k\|_2 = 1 \quad (1)$$

where $\mathbb{A} = \{1, 2, \dots, n_t\}$ is the spatial constellation symbol set. The signal constellation symbol comes from L -ary modulation, i.e., $s_k \in \mathbb{L}$, where \mathbb{L} is the signal constellation symbol set [e.g., 64 quadrature amplitude modulation (QAM)] of size L . Hence, each UL user's SM signal carries the information of $\log_2(L) + \log_2(n_t)$ bits per channel use (bpcu), and the overall UL throughput is $K(\log_2(L) + \log_2(n_t))$ bpcu. The users rely on the CPSC scheme for transmitting their SM signals [6]. Explicitly, each CPSC block consists of a cyclic prefix (CP) having the length of $P - 1$ and the associated data block having the length of Q . Hence, the length of each CPSC block is $Q + P - 1$, where this CP is capable of counteracting a dispersive multipath channel imposing dispersion over P samples. The concatenated data block consists of Q successive SM signals.

At the receiver, due to the reduced number of RF chains at the BS, only M_{RF} receive AEs can be exploited to receive signals, where existing receive AE selection schemes can be adopted to preselect M_{RF} receive AEs for achieving an improved signal detection performance [7]. Since the BS can serve K users simultaneously, after the removal of

187 the CP, the received signal $\mathbf{y}_q \in \mathbb{C}^{M_{\text{RF}}}$ for $1 \leq q \leq Q$ of the q th time
188 slot of a specific CPSC block can be expressed as

$$\mathbf{y}_q = \sum_{k=1}^K \mathbf{y}_{k,q} + \mathbf{w}_q = \sum_{p=0}^{P-1} \sum_{k=1}^K \mathbf{H}_{k,p} \Theta \mathbf{x}_{k,q} \bmod (q-p, Q) + \mathbf{w}_q \quad (2)$$

189 where $\mathbf{H}_{k,p} \in \mathbb{C}^{M \times n_t}$ is the k th user's MIMO channel matrix for the
190 p th multipath component, i.e., $\mathbf{H}_{k,p} \Theta = \tilde{\mathbf{H}}_{k,p} \in \mathbb{C}^{M_{\text{RF}} \times n_t}$; the set
191 Θ is determined by the AE selection scheme used; the elements of
192 Θ having the cardinality of M_{RF} are uniquely selected from the set
193 $\{1, 2, \dots, M\}$; $\mathbf{x}_{k,q}$ has one nonzero entry; and $\mathbf{w}_q \in \mathbb{C}^{M_{\text{RF}}}$ is the
194 additive white Gaussian noise (AWGN) vector with entries obeying
195 the independent and identically distributed (i.i.d.) circularly symmet-
196 ric complex Gaussian distribution with zero mean and a variance
197 of $\sigma_w^2/2$ per dimension, which is denoted by $\mathcal{CN}(0, \sigma_w^2)$. $\mathbf{H}_{k,p} =$
198 $\mathbf{R}_{\text{BS}}^{1/2} \tilde{\mathbf{H}}_{k,p} \mathbf{R}_{\text{US}}^{1/2}$, the entries of $\tilde{\mathbf{H}}_{k,p}$ obey the i.i.d. $\mathcal{CN}(0, 1)$, and
199 \mathbf{R}_{US} with the correlation coefficient ρ_{US} and \mathbf{R}_{BS} with the correlation
200 coefficient ρ_{BS} are correlation matrices at the users and the BS,
201 respectively. The specific element of the m th row and the n th column
202 of \mathbf{R}_{BS} (\mathbf{R}_{US}) is $\rho_{\text{BS}}^{|m-n|}$ ($\rho_{\text{US}}^{|m-n|}$). For correlated Rayleigh-fading
203 MIMO channels, the specific Θ or receive AE selection scheme has
204 an impact on the attainable system performance. In this paper, the
205 direct AE selection scheme is used for maximizing the minimum
206 geometric distance between any pair of the selected AEs [7]. For
207 uniform linear arrays (ULAs), $\Theta = \{\varphi + m_{\text{RF}} \lfloor M/M_{\text{RF}} \rfloor\}_{m_{\text{RF}}=0}^{M_{\text{RF}}-1}$
208 with $1 \leq \varphi \leq \lfloor M/M_{\text{RF}} \rfloor - 1$. Then, (2) can be further expressed as

$$\mathbf{y}_q = \sum_{p=0}^{P-1} \tilde{\mathbf{H}}_p \mathbf{x} \bmod (q-p, Q) + \mathbf{w}_q \quad (3)$$

209 by defining $\tilde{\mathbf{H}}_p = [\tilde{\mathbf{H}}_{1,p}, \tilde{\mathbf{H}}_{2,p}, \dots, \tilde{\mathbf{H}}_{K,p}] \in \mathbb{C}^{M_{\text{RF}} \times (n_t K)}$ and
210 $\mathbf{x}_q = [(\mathbf{x}_{1,q})^T, (\mathbf{x}_{2,q})^T, \dots, (\mathbf{x}_{K,q})^T]^T \in \mathbb{C}^{(n_t K)}$. By considering
211 the Q SM signals of a specific CPSC block, we arrive at

$$\mathbf{y} = \tilde{\mathbf{H}} \mathbf{x} + \mathbf{w} \quad (4)$$

212 where $\mathbf{y} = [(\mathbf{y}_1)^T, (\mathbf{y}_2)^T, \dots, (\mathbf{y}_Q)^T]^T \in (\mathbb{C}^{M_{\text{RF}} Q})$, the aggregate
213 SM signal $\mathbf{x} = [(\mathbf{x}_1)^T, (\mathbf{x}_2)^T, \dots, (\mathbf{x}_Q)^T]^T \in (\mathbb{C}^{(n_t K Q)})$, $\mathbf{w} =$
214 $[(\mathbf{w}_1)^T, (\mathbf{w}_2)^T, \dots, (\mathbf{w}_Q)^T]^T$, and

$$\tilde{\mathbf{H}} = \begin{bmatrix} \tilde{\mathbf{H}}_0 & \mathbf{0} & \mathbf{0} & \cdots & \tilde{\mathbf{H}}_2 & \tilde{\mathbf{H}}_1 \\ \tilde{\mathbf{H}}_1 & \tilde{\mathbf{H}}_0 & \mathbf{0} & \cdots & \vdots & \tilde{\mathbf{H}}_2 \\ \vdots & \tilde{\mathbf{H}}_1 & \tilde{\mathbf{H}}_0 & \cdots & \tilde{\mathbf{H}}_{P-1} & \vdots \\ \tilde{\mathbf{H}}_{P-1} & \vdots & \tilde{\mathbf{H}}_1 & \cdots & \mathbf{0} & \tilde{\mathbf{H}}_{P-1} \\ \mathbf{0} & \tilde{\mathbf{H}}_{P-1} & \vdots & \vdots & \vdots & \mathbf{0} \\ \vdots & \mathbf{0} & \tilde{\mathbf{H}}_{P-1} & \vdots & \vdots & \vdots \\ \vdots & \vdots & \mathbf{0} & \vdots & \mathbf{0} & \vdots \\ \vdots & \vdots & \vdots & \vdots & \tilde{\mathbf{H}}_0 & \mathbf{0} \\ \mathbf{0} & \mathbf{0} & \mathbf{0} & \cdots & \tilde{\mathbf{H}}_1 & \tilde{\mathbf{H}}_0 \end{bmatrix} \quad (5)$$

215 The signal-to-noise ratio (SNR) at the receiver is defined by $\text{SNR} =$
216 $E\{\|\tilde{\mathbf{H}} \mathbf{x}\|_2^2\} / E\{\|\mathbf{w}\|_2^2\}$.

The optimal signal detector for (4) relies on the ML algorithm, i.e., 217

$$\begin{aligned} \min_{\hat{\mathbf{x}}} \quad & \|\mathbf{y} - \tilde{\mathbf{H}} \hat{\mathbf{x}}\|_2 = \min_{\{\hat{\mathbf{x}}_{k,q}\}_{k=1, q=1}^{K, Q}} \|\mathbf{y} - \tilde{\mathbf{H}} \hat{\mathbf{x}}\|_2 \\ \text{s.t.} \quad & \text{supp}(\hat{\mathbf{x}}_{k,q}) \in \mathbb{A}, \hat{\mathbf{x}}_{k,q} \in \mathbb{L}, 1 \leq k \leq K, 1 \leq q \leq Q \end{aligned} \quad (6)$$

whose complexity exponentially increases with the number of users, 218
since the size of the search set for the ML detector is $(n_t \cdot L)^{KQ}$. 219
This excessive complexity can be unaffordable in practice. To reduce 220
the complexity, near-optimal sphere decoding detectors have been 221
proposed [10], but their complexity may still remain high, particularly 222
for the systems supporting large K , Q , n_t , and L [11]. In conventional 223
LS-MIMO systems, low-complexity linear signal detectors (e.g., the 224
MMSE-based signal detector) have been shown to be near optimal 225
since $M = M_{\text{RF}} \gg K$ and $n_t = 1$ make multiuser signal detection 226
an *overdetermined* problem [4]. However, in the proposed scheme, we 227
have $M_{\text{RF}} < K n_t$. Hence, the multiuser signal detection problem (6) 228
represents a large-scale *underdetermined* problem. Consequently, the 229
conventional linear signal detectors perform poorly in the proposed 230
LS-SM-MIMO [11]. By exploiting the sparsity of SM signals, the 231
authors in [11]–[13] have proposed the concept of CS-based signal 232
detectors for the downlink of small-scale SM-MIMO operating in a 233
single-user scenario. However, these signal detectors are unsuitable 234
for the proposed multiuser scenarios. Observe from (1) that $\mathbf{x}_{k,q}$ is 235
a sparse signal having a sparsity level of one. Hence, the aggregate 236
SM signal \mathbf{x} , which consists of multiple users' SM signals in Q 237
time slots, exhibits distributed sparsity with the sparsity level of KQ . 238
This property of \mathbf{x} inspires us to exploit the SCS theory for the 239
multiuser signal detection [14]. To further improve the signal detection 240
performance and to increase the system's throughput, we propose a 241
joint SM transmission scheme and an SCS-based MUD, which will be 242
detailed in the following section. 243

III. SCS-BASED MUD FOR LS-SM-MIMO UL 244

To solve the multiuser signal detection of our UL LS-SM-MIMO 245
system, we first propose a joint SM transmission scheme to be 246
employed at the users. Accordingly, an SCS-based low-complexity 247
MUD is developed at the BS, whereby the distributed sparsity of the 248
aggregate SM signal and the group sparsity of multiple aggregate SM 249
signals are exploited. Moreover, the computational complexity of the 250
proposed SCS-based MUD is discussed. 251

A. Joint SM Transmission Scheme at the Users 252

For the k th user in the q th time slot, every successive J CPSC block 253
is considered as a group, and they share the same spatial constellation 254
symbol, i.e., 255

$$\text{supp}(\mathbf{x}_{k,q}^{(1)}) = \text{supp}(\mathbf{x}_{k,q}^{(2)}) = \cdots = \text{supp}(\mathbf{x}_{k,q}^{(J)}), \quad 1 \leq k \leq K, 1 \leq q \leq Q \quad (7)$$

where we introduce the superscript (j) to denote the j th CPSC block, 256
and J is typically small, e.g., $J = 2$. In CS theory, the specific signal 257
structure, where $\mathbf{x}_{k,q}^{(1)}, \mathbf{x}_{k,q}^{(2)}, \dots, \mathbf{x}_{k,q}^{(J)}$ share a common support, is often 258
referred to as the *group sparsity*. Similarly, the aggregate SM signals 259
consisting of the K users' SM signals also exhibit group sparsity, i.e., 260

$$\text{supp}(\mathbf{x}^{(1)}) = \text{supp}(\mathbf{x}^{(2)}) = \cdots = \text{supp}(\mathbf{x}^{(J)}). \quad (8)$$

Although exhibiting group sparsity may slightly reduce the informa- 261
tion carried by the spatial constellation symbols, it is also capable of 262

reducing the number of the RF chains required according to the SCS theory, while simultaneously improving the total bit error rate (BER) of the entire system even with higher UL throughput. This conclusion will be confirmed by our simulation results.

B. SCS-Based MUD at the BS

According to (4), the received signals at the BS in the same group can be expressed as

$$\mathbf{y}^{(j)} = \tilde{\mathbf{H}}^{(j)} \mathbf{x}^{(j)} + \mathbf{w}^{(j)}, \quad 1 \leq j \leq J \quad (9)$$

where $\mathbf{y}^{(j)}$ denotes the received signal in the j th CPSC block, whereas $\tilde{\mathbf{H}}^{(j)}$ and $\mathbf{w}^{(j)}$ are the effective MIMO channel matrix and the AWGN vector, respectively.

The intrinsically distributed sparsity of $\mathbf{x}^{(j)}$ and the underdetermined nature of (9) inspire us to solve the signal detection problem based on CS theory, which can efficiently acquire the sparse solutions to underdetermined linear systems. Moreover, the J different aggregate SM signals in (9) can be jointly exploited for improving the signal detection performance due to the group sparsity of $\{\mathbf{x}^{(j)}\}_{j=1}^J$. Thus, by considering both the distributed sparsity and the group sparsity of the aggregate SM signals, the multiuser signal detection at the BS can be formulated as the following optimization problem:

$$\begin{aligned} \min_{\{\hat{\mathbf{x}}^{(j)}\}_{j=1}^J} \quad & \sum_{j=1}^J \|\mathbf{y}^{(j)} - \tilde{\mathbf{H}}^{(j)} \hat{\mathbf{x}}^{(j)}\|_2^2 = \min_{\{\hat{\mathbf{x}}_{k,q}^{(j)}\}_{j=1, k=1, q=1}^{J, K, Q}} \\ \sum_{j=1}^J \quad & \|\mathbf{y}^{(j)} - \tilde{\mathbf{H}}^{(j)} \hat{\mathbf{x}}^{(j)}\|_2^2 \\ \text{s.t.} \quad & \|\hat{\mathbf{x}}_{k,q}^{(j)}\|_0 = 1, \quad 1 \leq j \leq J, \quad 1 \leq q \leq Q, \quad 1 \leq k \leq K. \end{aligned} \quad (10)$$

Our proposed SCS-based MUD solves the optimization problem (10) with the aid of two steps. In the first step, we estimate the spatial constellation symbols, i.e., the indexes of K users' active AEs in J successive CPSC blocks. In the second step, we infer the legitimate signal constellation symbols of the K users in J CPSC blocks.

1. Step 1—Estimation of Spatial Constellation Symbols: We propose a group subspace pursuit (GSP) algorithm developed from the classical subspace pursuit (SP) algorithm in [15] to acquire the sparse solution to the large-scale underdetermined problem (10), where both the *a priori* sparse information (i.e., $\|\mathbf{x}_{k,q}^{(j)}\|_0 = 1$) and the group sparsity of $\mathbf{x}^{(1)}, \mathbf{x}^{(2)}, \dots, \mathbf{x}^{(J)}$ are exploited for improving the multiuser signal detection performance. The proposed GSP algorithm is described in **Algorithm 1**, which estimates SM signal $\{\hat{\mathbf{x}}_{k,q}^{(j)}\}_{k=1, j=1, q=1}^{K, J, Q}$. Hence, the estimated spatial constellation symbol is $\{\text{supp}(\hat{\mathbf{x}}_{k,q}^{(j)})\}_{k=1, j=1, q=1}^{K, J, Q}$.

Algorithm 1 Proposed GSP Algorithm.

Input: Noisy received signals $\mathbf{y}^{(j)}$ and effective channel matrices $\tilde{\mathbf{H}}^{(j)}$ for $1 \leq j \leq J$.

Output: Estimated $\hat{\mathbf{x}}^{(j)} = [(\hat{\mathbf{x}}_1^{(j)})^T, (\hat{\mathbf{x}}_2^{(j)})^T, \dots, (\hat{\mathbf{x}}_Q^{(j)})^T]^T$, where $\hat{\mathbf{x}}_q^{(j)} = [(\hat{\mathbf{x}}_{1,q}^{(j)})^T, (\hat{\mathbf{x}}_{2,q}^{(j)})^T, \dots, (\hat{\mathbf{x}}_{K,q}^{(j)})^T]^T$ for $1 \leq q \leq Q$.

1: $\mathbf{r}^{(j)} = \mathbf{y}^{(j)}$ for $1 \leq j \leq J$; {Initialization}

2: $\Omega^0 = \emptyset$; {Empty support set}

3: $t = 1$; {Iteration index}

4: **repeat** 304
 5: $\mathbf{a}_{k,q}^{(j)} = (\tilde{\mathbf{H}}_{k,q}^{(j)})^* \mathbf{r}^{(j)}$ for $1 \leq k \leq K$, $1 \leq q \leq Q$, and $1 \leq j \leq J$; 305
 {Correlation} 306
 6: $\tau_{k,q} = \arg \max_{\tau_{k,q}} \sum_{j=1}^J \|\mathbf{a}_{k,q}^{(j)}\|_2^2$ for $1 \leq k \leq K$, 307
 $1 \leq q \leq Q$; {Identify support} 308
 7: $\Gamma = \{\tau_{k,q} + (k-1 + K(q-1))n_t\}_{k=1, q=1}^{K, Q}$; {Preliminary 309
 support set} 310
 8: $\mathbf{b}^{(j)}|_{\Omega^{t-1} \cup \Gamma} = (\tilde{\mathbf{H}}^{(j)}|_{\Omega^{t-1} \cup \Gamma})^\dagger \mathbf{y}^{(j)}$ for $1 \leq j \leq J$; {Least 311
 squares} 312
 9: $\omega_{k,q} = \arg \max_{\omega_{k,q}} \sum_{j=1}^J \|\mathbf{b}_{k,q}^{(j)}\|_2^2$ for $1 \leq k \leq K$, 313
 $1 \leq q \leq Q$; {Pruning support set} 314
 10: $\Omega^t = \{\omega_{k,q} + (k-1 + K(q-1))n_t\}_{k=1, q=1}^{K, Q}$; {Final 315
 support set} 316
 11: $\mathbf{c}^{(j)}|_{\Omega^t} = (\tilde{\mathbf{H}}^{(j)}|_{\Omega^t})^\dagger \mathbf{y}^{(j)}$ for $1 \leq j \leq J$; {Least squares} 317
 12: $\mathbf{r}^{(j)} = \mathbf{y}^{(j)} - \tilde{\mathbf{H}}^{(j)} \mathbf{c}^{(j)}$ for $1 \leq j \leq J$; {Compute residual} 318
 13: $t = t + 1$; {Update iteration index} 319
 14: **until** $\Omega^t = \Omega^{t-1}$ or $t \geq Q$ 320

Compared with the classical SP algorithm, the proposed GSP algo- 321
 rithm exploits the distributed sparsity and group sparsity of $\{\mathbf{x}^{(j)}\}_{j=1}^J$. 322
 More explicitly, $\mathbf{x}^{(j)} \in \mathbb{C}^{(KQn_t)}$ consists of the KQ low-dimensional 323
 sparse vectors $\mathbf{x}_{k,q}^{(j)} \in \mathbb{C}^{n_t}$, where each $\mathbf{x}_{k,q}^{(j)}$ has the known sparsity 324
 level of one, and the aggregate SM signals $\mathbf{x}^{(1)}, \mathbf{x}^{(2)}, \dots, \mathbf{x}^{(J)}$ exhibit 325
 group sparsity. Specifically, the differences between the proposed GSP 326
 algorithm and the classical SP algorithm lie in the following two 327
 aspects: 1) the identification of the support set including the steps 328
 of the *preliminary support set* and the *final support set* as shown in 329
Algorithm 1; and 2) the joint processing of $\mathbf{y}^{(1)}, \mathbf{y}^{(2)}, \dots, \mathbf{y}^{(J)}$. First, 330
 for the support selection, taking the step of the *preliminary support set* 331
 for instance, when selecting the preliminary support set, the classical 332
 SP algorithm selects the support set associated with the first KQ 333
 largest values of the global correlation result $(\tilde{\mathbf{H}}^{(j)})^* \mathbf{r}^{(j)}$. By contrast, 334
 the proposed GSP algorithm selects the support set associated with 335
 the largest value from the local correlation result in each $(\tilde{\mathbf{H}}_{k,q}^{(j)})^* \mathbf{r}^{(j)}$. 336
 This way, the distributed sparsity of the aggregate SM signal can be ex- 337
 ploited for improved signal detection performance. Second, compared 338
 with the classical SP algorithm, the proposed GSP algorithm jointly 339
 exploits the J correlated signals having the group sparsity, which can 340
 bring the further improved signal detection performance. 341

It should be noted that even for the special case of $J = 1$, i.e., 342
 without using the joint SM transmission scheme, the proposed GSP 343
 algorithm still achieves a better signal detection performance than 344
 the classical SP algorithm when handling the aggregate SM signal, 345
 since the inherently distributed sparsity of the aggregate SM signal is 346
 leveraged to improve the signal detection performance. 347

2. Step 2—Acquisition of Signal Constellation Symbols: Following 348
Step 1, we can also acquire a rough estimate of the signal constellation 349
 symbol for each user in each time slot. By searching for the minimum 350
 Euclidean distance between this rough estimate of the signal constel- 351
 lation symbol and the legitimate constellation symbols of \mathbb{L} , we can 352
 obtain the final estimate of signal constellation symbols. 353

C. Computational Complexity

The optimal ML signal detector has a prohibitively high com- 355
 putational complexity of $\mathcal{O}((L \cdot n_t)^{(K \cdot Q)})$ according to (6). The 356
 sphere decoding detectors [10] are indeed capable of reducing the 357
 computational complexity, but they may still suffer from unaffordable 358
 complexity, particularly for large K, Q, L , and n_t values. By contrast, 359
 the conventional MMSE-based detector for LS-MIMO and CS-based 360

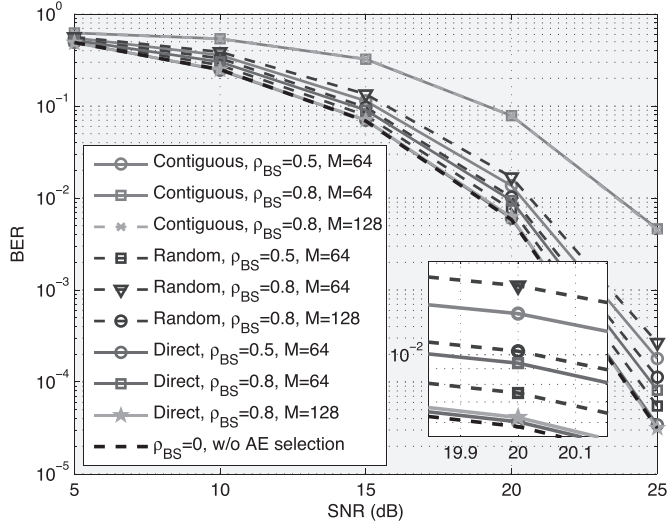


Fig. 2. Total BERs achieved by the proposed SCS-based MUD with different AE selection schemes, where $K = 8$, $J = 2$, 64-QAM, $M_{\text{RF}} = 18$, $n_t = 4$, and $\rho_{\text{US}} = 0$ are considered.

361 detector [13] for small-scale SM-MIMO enjoy the low complexity of
 362 $\mathcal{O}(M_{\text{RF}} \cdot (n_t \cdot Q \cdot K)^2 + (n_t \cdot Q \cdot K)^3)$ and $\mathcal{O}(2M_{\text{RF}} \cdot (Q \cdot K)^2 +$
 363 $(Q \cdot K)^3)$, respectively. For the proposed SCS-based MUD, most
 364 of the computational requirements are imposed by the least squares
 365 (LS) operations, which has complexity of $\mathcal{O}(J \cdot (2M_{\text{RF}} \cdot (Q \cdot K)^2 +$
 366 $(Q \cdot K)^3))$ [16]. Consequently, the computational complexity per
 367 CPSC block is $\mathcal{O}(2M_{\text{RF}} \cdot (Q \cdot K)^2 + (Q \cdot K)^3)$, since J successive
 368 aggregate SM signals are jointly processed. Compared with conven-
 369 tional signal detectors, the proposed SCS-based MUD benefits from
 370 substantially lower complexity, and it has similar low complexity as
 371 the conventional MMSE- and CS-based signal detectors.

IV. SIMULATION RESULTS

373 A simulation study was carried out to compare the attainable perfor-
 374 mance of the proposed SCS-based MUD to that of the MMSE-based
 375 signal detector [4] and to that of the CS-based signal detector [13].
 376 In the LS-SM-MIMO system considered, the BS used a ULA relying
 377 on a large number of AEs M , but a much smaller number of RF
 378 chains M_{RF} , whereas K users employing n_t AEs but only a single RF
 379 chain simultaneously use the CPSC scheme associated with $P = 8$ and
 380 $Q = 64$ to transmit the SM signals to the BS. The total BER including
 381 both the spatial constellation symbols and the signal constellation
 382 symbols was evaluated.

383 Fig. 2 compares the total BERs achieved by the proposed SCS-based
 384 MUD with different AE selection schemes, where $K = 8$, $J = 2$,
 385 64-QAM, $M_{\text{RF}} = 18$, $n_t = 4$, and $\rho_{\text{US}} = 0$ are considered. The con-
 386 tiguous AE selection scheme implies that we select M_{RF} adjacent
 387 AEs, i.e., $\Theta = \{\varphi + m_{\text{RF}}\}_{m_{\text{RF}}=0}^{M_{\text{RF}}-1}$ with $1 \leq \varphi \leq M - M_{\text{RF}} + 1$. By
 388 contrast, in the random AE selection scheme, the elements of Θ are
 389 randomly selected from the set $\{1, 2, \dots, M\}$, whereas the direct
 390 AE selection scheme in [7] has been described in Section II-B.
 391 Furthermore, the BER achieved by the SCS-based MUD relying on
 392 $\rho_{\text{BS}} = 0$ is also considered as a performance bound, since the choice
 393 of $\rho_{\text{BS}} = 0$ and $\rho_{\text{US}} = 0$ implies the uncorrelated Rayleigh-fading
 394 MIMO channels. Observe from Fig. 2 that the direct AE selection
 395 scheme outperforms the other pair of AE selection schemes. Moreover,
 396 for a certain AE selection scheme, the BER performance degrades
 397 when M_{RF}/M or ρ_{BS} increases. For the direct AE selection scheme,
 398 the BER performance of $\rho_{\text{BS}} = 0.8$, $M = 128$ and of $\rho_{\text{BS}} = 0.5$,

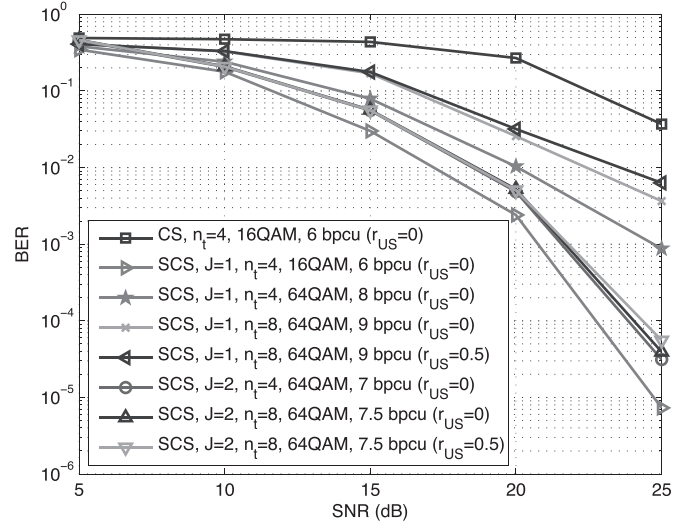


Fig. 3. Total BERs achieved by the CS-based signal detector and the SCS-based MUD against different SNRs in LS-SM-MIMO, where $K = 8$, $M_{\text{RF}} = 18$, $M = 64$, $\rho_{\text{BS}} = 0.5$, and the direct AE selection scheme is considered.

$M = 64$ approaches the BER achieved for transmission over uncor- 399
 related Rayleigh-fading MIMO channels, which confirms the near- 400
 optimal performance of the direct AE selection scheme. 401

Fig. 3 compares the overall BER achieved by the CS-based signal 402
 detector and by the proposed SCS-based MUD versus the SNR in our 403
 LS-SM-MIMO context, where $K = 8$, $M_{\text{RF}} = 18$, $M = 64$, $\rho_{\text{BS}} = 0.5$, and the direct AE selection scheme is considered. The SCS-based 405
 MUD outperforms the CS-based signal detector even for $J = 1$, since 406
 the distributed sparsity of the aggregate SM signal is exploited. For the 407
 SCS-based MUD, the BER performance improves when J increases, 408
 albeit this is achieved at the cost of reduced UL throughput. To mitigate 409
 this impediment, a higher number of AEs can be employed by the users 410
 for expanding the spatial constellation symbol set constituted by the 411
 AEs. Specifically, by increasing n_t from 4 to 8, the UL throughput 412
 of the SCS-based MUD may be increased, but having more AEs at 413
 the user results in a higher ρ_{US} . When n_t is increased, the BER 414
 performance of the SCS-based MUD associated with $J = 1$ degrades, 415
 as expected. By contrast, when n_t is increased, the BER performance 416
 loss of the SCS-based MUD using $J = 2$ can be less than 0.2 dB if the 417
 BER of 10^{-4} is considered, even when a higher ρ_{US} associated with a 418
 higher n_t is considered. 419

Fig. 4 portrays the BER achieved by the different signal detectors as 420
 a function of the SNR in the context of the proposed LS-SM-MIMO 421
 for $K = 8$, $M_{\text{RF}} = 18$, $M = 64$, $n_t = 4$, $\rho_{\text{BS}} = 0.5$, and $\rho_{\text{US}} = 0$, 422
 where the direct AE selection scheme is also considered. In Fig. 4, 423
 we also characterize the ‘oracle-assisted’ LS-based signal detector 424
 relying on the assumption that the spatial constellation symbol is 425
 perfectly known at the BS for the proposed LS-SM-MIMO scheme 426
 associated with $J = 2$, 64-QAM as well as for the MMSE-based 427
 LS-MIMO detector in conjunction with 64-QAM, where both of them 428
 only consider the BER of the classic signal constellation symbol. Here, 429
 we assume that the LS-MIMO arrangement uses the same number 430
 of RF chains to serve eight single-antenna users communicating 431
 over uncorrelated Rayleigh-fading channels. The superiority of our 432
 SCS-based MUD over the MMSE- and CS-based signal detectors 433
 becomes clear. 434

Moreover, the performance gap between the oracle LS-based signal 435
 detector associated with 7 bpcu and the proposed SCS-based MUD 436
 with 7 bpcu is less than 0.5 dB. Note again that the oracle LS-based sig- 437
 nal detector only considers the BER of the classic signal constellation 438

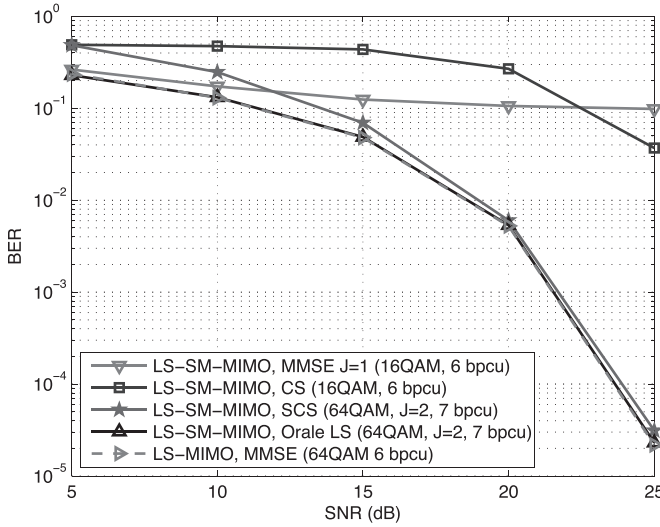


Fig. 4. Total BERs achieved by different signal detectors against different SNRs in the proposed LS-SM-MIMO and conventional LS-MIMO.

symbol, whereas the proposed SCS-based MUD considers both the spatial and the classic signal constellation symbols. Finally, compared with the conventional LS-MIMO using the MMSE-based signal detector (6 bpcu), our proposed UL LS-SM-MIMO and the associated SCS-based MUD (7 bpcu) only suffer from a negligible BER loss, which explicitly confirmed the improved UL throughput of the proposed LS-SM-MIMO scheme.

V. CONCLUSION

We have proposed an LS-SM-MIMO scheme for the UL transmission. The BS employs a large number of AEs but a much smaller number of RF chains, where a simple receive AE selection scheme is used for the improved performance. Each user equipped with multiple AEs but only a single RF chain uses CPSC to combat multipath channels. SM has been adopted for the UL transmission to improve the UL throughput. The proposed scheme is particularly suitable for scenarios where a large number of low-cost AEs can be accommodated, and both power consumption and hardware cost are heavily determined by the number of RF chains. Due to the reduced number of RF chains at the BS and multiple AEs employed by each user, the UL multiuser signal detection is a challenging large-scale underdetermined problem. We have proposed a joint SM transmission scheme at the users to introduce the group sparsity of multiple aggregate SM signals, and a

matching SCS-based MUD at the BS has been proposed to leverage the inherently distributed sparsity of the aggregate SM signal as well as the group sparsity of multiple aggregate SM signals for reliable multiuser signal detection performance. The proposed SCS-based MUD enjoys the low complexity, and our simulation results have demonstrated that it performs better than its conventional counterparts with even much higher UL throughput.

REFERENCES

- [1] M. D. Renzo, H. Haas, A. Ghayeb, S. Sugiura, and L. Hanzo, "Spatial modulation for generalized MIMO: Challenges, opportunities and implementation," *Proc. IEEE*, vol. 102, no. 1, pp. 56–103, Jan. 2014.
- [2] A. Younis, R. Mesleh, M. Di Renzo, and H. Haas, "Generalised spatial modulation for large-scale MIMO," in *Proc. EUSIPCO*, Sep. 2014, pp. 346–350.
- [3] S. Ganesan, R. Mesleh, H. Haas, C. Ahn, and S. Yun, "On the performance of spatial modulation OFDM," in *Proc. 40th Asilomar Conf. Signals, Syst. Comput.*, Oct. 2006, pp. 1825–1829.
- [4] F. Rusek *et al.*, "Scaling up MIMO: Opportunities and challenges with very large arrays," *IEEE Signal Process. Mag.*, vol. 30, no. 1, pp. 40–60, Jan. 2013.
- [5] N. Serafimovski *et al.*, "Practical implementation of spatial modulation," *IEEE Trans. Veh. Technol.*, vol. 62, no. 9, pp. 4511–4523, Nov. 2013.
- [6] P. Som and A. Chockalingam, "Spatial modulation and space shift keying in single carrier" in *Proc. IEEE Int. Symp. PIMRC*, Sep. 2012, pp. 1062–1067.
- [7] X. Wu, M. Di Renzo, and H. Haas, "Adaptive selection of antennas for optimum transmission in spatial modulation," *IEEE Trans. Wireless Commun.*, vol. 14, no. 7, pp. 3630–3641, Jul. 2015.
- [8] S. Narayanan *et al.*, "Multi-user spatial modulation MIMO" in *Proc. IEEE WCNC*, Apr. 2014, pp. 671–676.
- [9] X. Wu, H. Claussen, M. D. Renzo, and H. Haas, "Channel estimation for spatial modulation," *IEEE Trans. Commun.*, vol. 62, no. 12, pp. 4362–4372, Dec. 2014.
- [10] A. Younis, S. Sinanovic, M. Di Renzo, R. Mesleh, and H. Haas, "Generalised sphere decoding for spatial modulation," *IEEE Trans. Commun.*, vol. 61, no. 7, pp. 2805–2815, Jul. 2013.
- [11] W. Liu, N. Wang, M. Jin, and H. Xu, "Denoising detection for the generalized spatial modulation system using sparse property," *IEEE Commun. Lett.*, vol. 18, no. 1, pp. 22–25, Jan. 2014.
- [12] B. Shim, S. Kwon, and B. Song, "Sparse detection with integer constraint using multipath matching pursuit," *IEEE Commun. Lett.*, vol. 18, no. 10, pp. 1851–1854, Oct. 2014.
- [13] C. Yu *et al.*, "Compressed sensing detector design for space shift keying in MIMO systems," *IEEE Commun. Lett.*, vol. 16, no. 10, pp. 1556–1559, Oct. 2012.
- [14] M. F. Duarte and Y. C. Eldar, "Structured compressed sensing: From theory to applications," *IEEE Trans. Signal Process.*, vol. 59, no. 9, pp. 4053–4085, Sep. 2011.
- [15] W. Dai and O. Milenkovic, "Subspace pursuit for compressive sensing signal reconstruction," *IEEE Trans. Inf. Theory*, vol. 55, no. 5, pp. 2230–2249, May 2009.
- [16] A. Björck, *Numerical Methods for Matrix Computations*. Cham, Switzerland: Springer Int. Publ. AG, 2014.

AUTHOR QUERY

NO QUERY.